Kristensen et al. Geotherm Energy (2016) 4:6
DOI 10.1186/s40517-016-0048-6

Geothermal Energy

RESEARCH

Open Access

Pre-drilling assessments of average porosity and permeability in the geothermal reservoirs of the Danish area

Lars Kristensen[1*], Morten Leth Hjuler[1], Peter Frykman[1], Mette Olivarius[1,2], Rikke Weibel[1], Lars Henrik Nielsen[1] and Anders Mathiesen[1]

*Correspondence: lk@geus.dk
[1] Geological Survey of Denmark and Greenland (GEUS), Øster Voldgade 10, 1350 Copenhagen, Denmark
Full list of author information is available at the end of the article

Abstract

Denmark constitutes a low-enthalpy geothermal area, and currently geothermal production takes places from two sandstone-rich formations: the Bunter Sandstone and the Gassum formations. These formations form major geothermal reservoirs in the Danish area, but exploration is associated with high geological uncertainty and information about reservoir permeability is difficult to obtain. Prediction of porosity and permeability prior to drilling is therefore essential in order to reduce risks. Geologically these two formations represent excellent examples of sandstone diversity, since they were deposited in a variety of environments during arid and humid climatic conditions. The study is based on geological and petrophysical data acquired in deep wells onshore Denmark, including conventional core analysis data and well-logs. A method for assessing and predicting the average porosity and permeability of geothermal prospects within the Danish area is presented. Firstly, a porosity-depth trend is established in order to predict porosity. Subsequently, in order to predict permeability, a porosity–permeability relation is established and then refined in steps. Both one basin-wide and one local permeability model are generated. Two porosity-depth models are established. It is shown that the average permeability of a geothermal prospect can be modelled (predicted) using a local permeability model, i.e. a model valid for a geological province including the prospect. The local permeability model is related to a general permeability model through a constant, and the general model thus acts as a template. The applied averaging technique reduces the scatter that is normally seen in a porosity–permeability plot including all raw core analysis measurements and thus narrows the uncertainty band attached to the average permeability estimate for a reservoir layer. A "best practice" technique for predicting average porosity and permeability of geothermal prospects on the basis of core analysis data and well-logs is suggested. The porosity is primarily related to depth, whereas the permeability also depends on porosity, mineralogy and grain size, which are controlled by the depositional environment. Our results indicate that porosity and permeability assessments should be based on averaged data and not raw conventional core analysis data. The uncertainty range of permeability values is significantly lower, when average values are used.

Keywords: Geothermal reservoirs, Porosity, Permeability, Reservoir quality, Diagenesis, Prediction of reservoir parameters, Averaging technique, Variability

Background

Recent evaluations of seismic reflection surveys and well data acquired during former geothermal and hydrocarbon exploration activities indicate that several sandstone-rich formations in the Norwegian-Danish Basin and the North German Basin contain substantial geothermal low-enthalpy resources (Mathiesen et al. 2009; Norden 2011; Kirsch et al. 2015). These basins are classic sedimentary basins characterized by long-term subsidence and infilling by sediments (Bertelsen 1980; Nielsen 2003; Bachmann et al. 2010; Lott et al. 2010). The geothermal potential of the Danish area has been addressed by GEUS in a regional assessment to the Danish Energy Agency and in a large number of customer reports prepared for district heating companies during the last 10 years (e.g. Hjuler et al. 2014; Mathiesen et al. 2010a, b). Furthermore, GEUS has evaluated and assessed the geothermal potential of selected city areas in Denmark. These activities are reviewed in Mathiesen et al. (2010b) and Vosgerau et al. (in press).

In the Norwegian-Danish Basin and the North German Basin, the widely distributed Bunter Sandstone and Gassum formations constitute major geothermal reservoirs, but also formations with more local distribution, such as Skagerrak, Haldager Sand, Flyvbjerg and Frederikshavn formations, have geothermal potentials (Røgen et al. 2015; Mathiesen et al. 2010b, Nielsen et al. 2004). The geothermal potential is related directly to reservoir quality, which in the Danish onshore area traditionally is addressed by considering clay content, net sand thickness, porosity and permeability by means of wireline logs, core analysis data, well tests and seismic data (e.g. Mathiesen et al. 2013). The available seismic and well data point to thick reservoir formations and in addition, formation temperatures, porosities and permeabilities have proven to be sufficiently high for geothermal water production in large parts of Denmark.

Denmark is a low-enthalpy geothermal area with a temperature gradient of 25–30 °C/km, and only minor temperature anomalies are encountered in the subsurface (Balling et al. 1981; Mathiesen et al. 2013; Balling et al. 2014; Poulsen et al. submitted). The geothermal potential onshore Denmark has been mapped for the Bunter Sandstone (including Skagerrak), Gassum, Haldager Sand and Frederikshavn formations (Mathiesen et al. 2009, 2010b). The mapping considered distribution and estimated resources of these formations, and potential geothermal reservoirs were identified as sandstone layers having thicknesses greater than 25 m in the depth interval 800–3000 m, corresponding to formation temperatures in the range 25–100 °C. The permeability in deeper-seated reservoirs is considered too low for geothermal water production (Mathiesen et al. 2009, 2010b; Weibel et al. submitted). Presently, two plants produce from the Gassum formation; saline water (43 °C) is produced from a depth of 1250 m at Thisted, whereas water of 48 °C is produced at Sønderborg (depth 1200 m). At a plant in Copenhagen ('Margretheholm'), saline water (74 °C) is produced from the Bunter Sandstone formation located at a depth of c. 2600 m (Røgen et al. 2015). Each plant is configured with a production well and an injection well located about 1 km from the producer, returns the cooled water.

A prognosis (pre-drilling assessment) of reservoir porosity and permeability for the three Danish geothermal plants was not carried out in a quantitative fashion, but the intention of this paper is to suggest a methodology that makes it possible to predict reservoir properties of new geothermal prospects, as the lack of accurate predictions is regarded as the 'bottle-neck' for new projects. In contrast, the depth, thickness and temperature can in most areas be estimated with an uncertainty of less than 10 %. Our work thus aims at presenting a method for assessing the average porosity and permeability of geothermal prospects within the Danish area. The method is considered a "best practice" approach.

Especially in poorly explored regions, prediction of reservoir parameters along with an assessment of the geological development is needed prior to drilling. Pre-drilling assessments of uncertainties and general reservoir parameters (thickness, porosity, permeability and temperature) are crucial for estimating the geothermal potential in such areas. Seismic interpretation is essential in order to determine depth and thicknesses. Setting up a work programme for a geothermal project thus requires a careful integration of existing geological and geophysical information.

The present study is based on geological and petrophysical data acquired in deep wells onshore Denmark. The database is comprehensive and it contains widely distributed data, both vertically and geographically. However, the data density varies considerably; both closely spaced and sporadically distributed data form part of the database. A statistical approach to data analysis is not feasible when dealing with such a database with large variations in data density and distribution. As an alternative the data analysis is herein based on an empirical approach. Two porosity-depth trends along with a number of empirical porosity–permeability relationships that are established using existing well-logs and core analysis data, and then used for reservoir characterization. These trends and relations are considered to have a predictive potential and may be used for characterizing a geothermal prospect, provided that the approximate depth to the anticipated geothermal reservoir is known. Our empirical porosity–permeability trends are established on the basis of core analysis data available from wells drilled and cored during the period *c.* 1950–2010. The large time span implies that quality of core analysis data, i.e. porosity and permeability measurements on plug samples, varies considerably but generally the quality is fair to good. The data material indicates that the correspondence between core porosity and core permeability data is not perfect, but reasonable porosity–permeability correlations may be obtained, despite the rather scattered data. As permeability can be predicted with least confidence, the main emphasis is laid on improving permeability prediction in areas with sparse data coverage.

With respect to geothermal exploration in the Danish onshore area, two issues are particularly important for the local district heating companies holding the geothermal exploration license areas: (1) the geological uncertainty prior to drilling the first well needs to be thoroughly assessed and (2) the prognosis for permeability and transmissivity in a potential reservoir needs to be as well constrained as possible. In some cases it has been concluded that the geological uncertainty and the associated exploration risks are too high for justifying the drilling of the first and costly geothermal exploration well.

Previous studies of relevance

Many workers have discussed the correlation between porosity and permeability measurements, and despite somewhat imperfect correlations, they succeeded in establishing either exponential relationships (e.g. Tiab and Donaldson 2004) or trends defined by power functions (e.g. Doyen 1988; Mavko and Nur 1997).

A number of methods for determining permeability from porosity are described in literature, including empirical approaches and various modelling techniques. Already in 1927, Kozeny proposed to predict permeability from porosity, geometry of the pores and the specific surface of the solids in contact with the fluid. The Kozeny equation was later modified by Carman (1937, 1956) to become the Kozeny–Carman equation, which estimates the permeability of a porous media based on a grain size distribution. Block (1991) outlined a predictive approach based on the correlation between porosity and permeability in which the predictive applicability is constrained by the limits defined by a calibration dataset that includes various petrographic variables or parameters. Block (1991) even provided an equation in which the permeability is expressed as a function of grain size, sorting and rigid grain content. Evans et al. (1997) discussed a permeability prediction methodology that is based on a combination of empirical and geological modelling approaches. Originally the Kozeny equation was derived for clay-free sand with high porosity, and for that reason Walderhaug et al. (2012) suggested a modified Kozeny equation for predicting permeability in quartz-rich sandstones, even with high clay content. This modified Kozeny equation includes a parameter reflecting the type of pore system, and usually this parameter is to be considered a constant for a specific sandstone unit. With respect to modelling, Vadapalli et al. (2014) present fractal and Monte Carlo simulation approaches for permeability prediction.

Porosity and permeability assessments

Our porosity modelling is based on data from the Bunter Sandstone and Gassum formations. The permeability modelling is demonstrated by data from the Gassum formation.

Quantification of reservoir permeability, which is the single most critical factor for geothermal fluid extraction, is complicated as very few in situ measurements are available and moreover, permeability logs are not available from wells in the Danish onshore area.

Determination of reservoir permeability requires good-quality well test data, i.e. tests based on sufficiently long test intervals and flow/build-up periods of long duration. However, such high-quality test data only exist for a few Danish onshore wells (e.g. at Stenlille and Tønder; Fig. 1), and well test data are generally not available. So as an alternative, it is suggested to assess the permeability from an analysis of porosity log data supplemented by information from porosity–permeability relationships based on core analysis data. Core analysis data commonly include gas permeabilities measured at laboratory conditions, but conversion into corresponding reservoir fluid permeabilities (at field scale) is not a straightforward task. This conversion normally involves transformation of the core scale gas permeability into liquid permeability followed by upscaling from laboratory scale to field scale. The correction from gas to liquid permeability is normally carried out as a Klinkenberg correction of laboratory measurements (Klinkenberg 1941). The Klinkenberg correction is quite important for low-permeability sandstones, where a factor of 0.5 may apply, but for high permeabilities (>100 mD) the Klinkenberg correction is less pronounced and a factor in the order of 0.8–0.9 may apply (Tanikawa and Shimamoto 2009; Duan and Yang 2014). The use of core permeability values for upscaling to a full reservoir volume assumes that the sampling of the core samples is representative, which is not always the case. The arithmetic averaging used

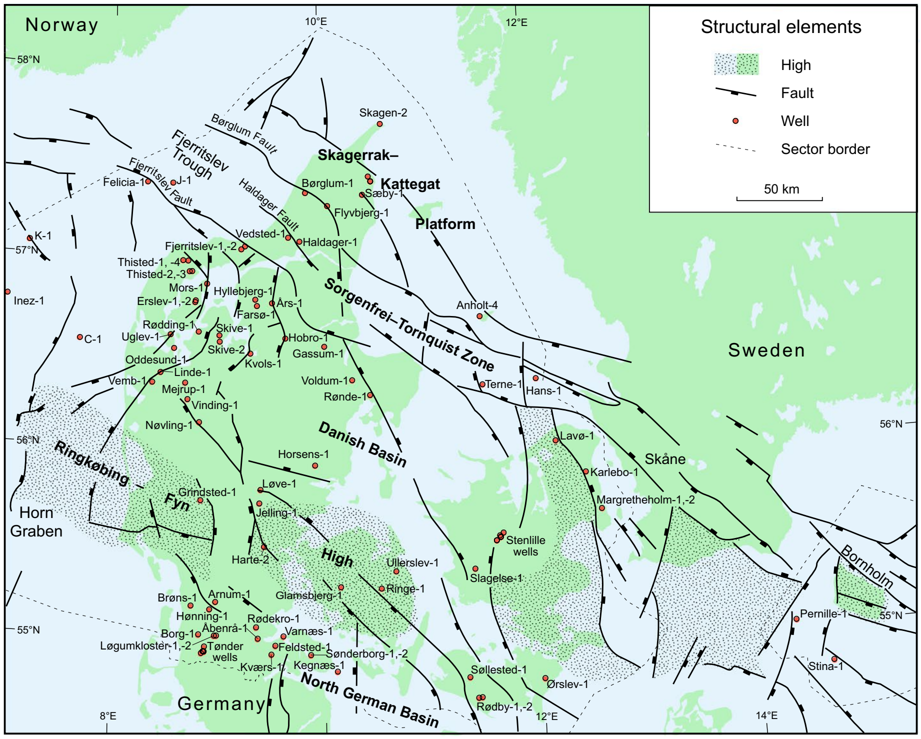

Fig. 1 Well locations and principal structural elements in the Danish area. The positions of the Ringkøbing–Fyn High, the Danish part of the Norwegian-Danish Basin and the northern part of the North German Basin are shown. In addition, the location of the Sorgenfrei–Tornquist Zone and the Skagerrak–Kattegat platform is shown. Danish onshore wells and selected offshore wells relevant for geothermal exploration are *plotted*

herein is based on the concept of horizontal, along layer flow, and occurring in a layered formation, which has been shown to be closely comparable to that from more advanced upscaling schemes (Kazemi et al. 2012).

The Danish onshore core analysis database is considerably larger than the number of well tests, and the purpose of analysing core permeability data is to provide an estimate of the average permeability that characterizes a particular layer, but also to address the uncertainty of a predicted permeability estimate. A single permeability value interpreted from well test data is, however, not directly comparable to an average permeability based on core data, but the two permeability assessments are comparable at a relative scale, on the assumption that the thickness of test interval corresponds to the length of the cored interval.

Geological setting

The Norwegian-Danish Basin contains a thick Upper Permian–Mesozoic succession of sedimentary rocks (Fig. 1). The basin was formed in Late Carboniferous–Early Permian time by crustal stretching, succeeded by deposition of Rotliegendes coarse-grained clastic sediments and later by Zechstein salts (Stemmerik et al. 1987; Nielsen 2003; Vejbæk 1989, 1997; Michelsen and Nielsen 1993; Pharaoh et al. 2010). The Permian period followed basinal subsidence governed primarily by thermal cooling and local faulting, and the Triassic sediments include a succession of sandstones, mudstones, carbonates and evaporites, whereas the Jurassic strata are dominated by mudstones and sandstones (Berthelsen 1980; Michelsen and Clausen 2002; Nielsen 2003). The Mesozoic deposition is influenced by differential uplift across the basin and occasionally, halokinesis has resulted in local deviations from the regional uplift trend (Japsen et al. 2007). The regional trend points to gradually increasing uplift toward the northeast. The Cretaceous sediments encompass limestones, mudstones, sandstones, marls and chalks. The Cenozoic succession comprises a series of primarily mudstones, sandstones and limestones.

Bunter sandstone formation

The Lower Triassic Bunter sandstone formation is widely distributed in the North German Basin and in parts of the Norwegian-Danish Basin (Fig. 2) (Berthelsen 1980; Nielsen and Japsen 1991; Michelsen and Clausen 2002; Bachmann et al. 2010). In Denmark, this formation is especially relevant for geothermal exploration in the southern and eastern parts of the country due to sufficient thickness and generally good reservoir properties (Mathiesen et al. 2010a, b). Formation thickness varies from about 300 m in the Margretheholm wells in the eastern part of the Norwegian-Danish Basin to 600–700 m in the central parts of the basin and to *c.* 200 m in the Tønder wells in the North German Basin (Fig. 1). In general the formation thins towards the Ringkøbing–Fyn High, and it is locally absent on the High (Nielsen and Japsen 1991; Olivarius et al. 2015b). The reservoir quality of the formation varies considerably, as the lithology varies from sandstones with a subordinate amount of mudstones, to siltstones and mudstones with few sandstone layers (Berthelsen 1980; Clemmensen 1985). However, the reservoir quality of the thickest sandstone layers is generally good to excellent (Olivarius et al. 2015a). The Bunter Sandstone formation was deposited in an arid to semi-arid climate, and the sandstones represent deposition by fluvial channel systems and eolian dunes, whereas the mudstones mainly were deposited in lakes and on flood plains (Clemmensen 1985). Eroded material was supplied from the Ringkøbing–Fyn High by alluvial–fluvial systems and by wind transport across the North German Basin (Olivarius et al. 2015b; Clausen and Pedersen 1999).The sandstone layers are generally continuous, especially the eolian sandstones, and consist mostly of very fine to medium-grained sand (Olivarius et al. 2015b). Similarly, eroded material from the Fennoscandian Shield was transported into the Danish Basin (Bertelsen 1980; Olivarius and Nielsen 2016). The sandstone deposits are fine to coarse grained and generally, grain size increases in a northeasterly direction, i.e. towards the flanks of the basin. In the southern and central parts of the Danish Basin, the deposits belong to the Bunter Sandstone formation and to the Skagerrak formation in the northeastern part.

Gassum formation

The Upper Triassic–Lower Jurassic Gassum formation is present in most of the Norwegian-Danish Basin (Fig. 2), except above large salt structures and on the Ringkøbing–Fyn High (Nielsen 2003). It is also present in the northern North German Basin, but here its patchy and shallow occurrence makes it less suitable for geothermal exploration. In general, the formation thickness varies from *c.* 30 m to more than 300 m (Michelsen et al. 2003). Nielsen (2003) described the geological development of the Gassum formation in detail: the formation consists of shallow marine, fluvial and estuarine sandstones

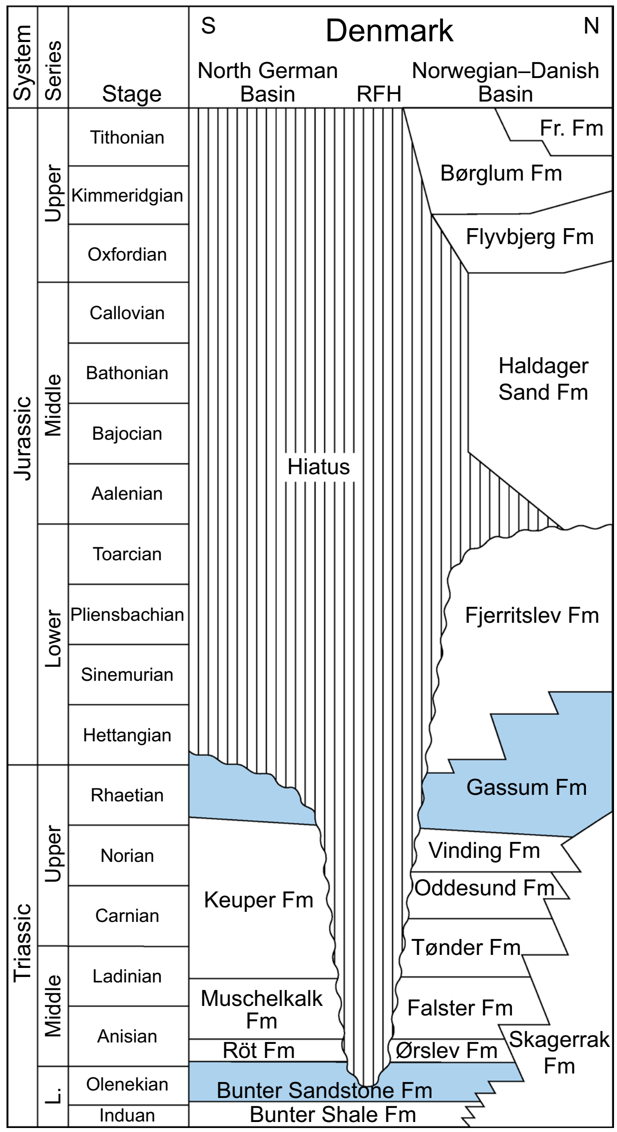

Fig. 2 A North–South trending lithostratigraphic scheme. The scheme encompasses the Norwegian-Danish Basin and the North German Basin, including the widely distributed Lower Triassic Bunter Sandstone and Upper Triassic–Lower Jurassic Gassum formations (highlighted in *blue*). The scheme is based on data from Berthelsen (1980), Michelsen and Clausen (2002) and Nielsen (2003). The pronounced hiatus centred over the Ringkøbing–Fyn High illustrates the uplift and erosion that occurred mainly in Middle Jurassic time (Nielsen 2003). The Bunter sandstone and Gassum formations constitute major geothermal reservoirs, but also the more locally distributed Skagerrak, Haldager Sand, Flyvbjerg and Frederikshavn formations have geothermal potentials. *RFH* Ringkøbing–Fyn High

interbedded with marine and lagoonal mudstones, and also siltstones and minor coal beds are present. During the Late Triassic to Early Jurassic, the sedimentation was influenced by repeated sea-level fluctuations and rivers transported eroded material from the Fennoscandian Shield into the Norwegian-Danish Basin. Several sandstone layers were deposited as regressive shoreface sands, but also as fluvial sands deposited in river channels or estuaries. The Gassum formation was deposited in a humid climate, and the sandstone layers consist mainly of fine to medium-grained sand. The mudstones were primarily deposited in lagoons, lakes and offshore shelf areas. The reservoir quality of the sandstones is generally good to excellent due to the presence of rather continuous sandstone beds with low clay content (Weibel et al. submitted).

The influence of diagenesis on reservoir quality

The porosity and permeability of the Bunter Sandstone and Gassum formations generally decrease with increasing burial depth, due to mechanical compaction and diagenetic alterations (Olivarius et al. 2015a, b; Weibel et al. submitted). Diagenesis (e.g. cementation) may even affect the sandstones at shallow burial, but otherwise mechanical compaction is dominant at shallow burial (Table 1). Chemical compaction becomes more pronounced at depths greater than 2–3 km owing to higher temperature and pressure. Quartz cement is considered the major porosity reducing element in quartz-dominated sandstones at depth greater than 2000 m (Ehrenberg 1990). The sandstones of the Gassum formation are affected by pronounced quartz cementation at greater depths, but also the presence of carbonate cement (calcite, siderite and ankerite) and clays affects reservoir quality as well (Weibel et al. submitted). In the Bunter Sandstone formation quartz cementation is very limited due to shallow burial, so the reservoir quality is mainly influenced by calcite, anhydrite and halite cements along with clay minerals (Olivarius et al. 2015a). This difference in the diagenetic development of the Bunter Sandstone and Gassum formations may be attributed to the differences in the depositional environments caused by the different climatic conditions during deposition, i.e. arid conditions versus humid conditions (see Olivarius et al. 2015a and Weibel et al. submitted).

In general, the permeability reduction with burial depth is more pronounced for fine-grained sandstones than for coarse grained, but also the content of detrital clay, sorting and other elements related to variations in the depositional environments and source area proximity affect permeability (Weibel et al. submitted; Olivarius et al. 2015a, b). The presence of diagenetic cements may result in substantial permeability reduction, as the cement reduces the size of the pore throats. A synopsis of the key factors affecting porosity and permeability compiled from Olivarius et al. (2015a) and Weibel et al. (submitted) is presented in Table 1, covering both the Bunter Sandstone and Gassum formations. The tabulation summarizes the results of two diagenesis studies based on analyses of thin sections, scanning electron microscope images, cores and cuttings samples.

Methods

A 5-step procedure has been developed in order to improve predictions of reservoir parameters valid for geothermal prospects in areas with poor data coverage, i.e. areas with no wells, but with sufficient seismic data to determine approximate depths and thicknesses of potential reservoirs.

- First step is to establish a regional model for porosity prediction.
- In step 2, a permeability model is established.
- In step 3, the permeability model is refined.
- Step 4 includes the establishment of local permeability models.
- Step 5 is implemented to reduce the uncertainty range of the permeability.

Table 1 Factors influencing porosity and permeability in the Bunter Sandstone and Gassum formations

Factors	Depth <2500 m	Depth >2500 m
Depth (max. burial depth)	*Bunter Sandstone Fm* Mechanical compaction. Core data represent a narrow depth interval *Gassum Fm* Mechanical compaction. The porosity reduction with depth is comparable to the porosity estimated from a mechanical compaction curve. Depth is an important factor, when dealing with permeabilities of shallowly buried sandstones	*Bunter Sandstone Fm* No core data *Gassum Fm* Chemical compaction. The porosity reduction with depth may be higher than indicated by a mechanical compaction curve. Permeability is not that depth dependent
Grain size	*Bunter Sandstone Fm* Porosity reduction is highest for very fine-grained sandstones and less for coarser-grained sandstones. Increasing grain size leads to higher permeabilities *Gassum Fm* Limited influence on porosity. Increasing grain size leads to higher permeabilities	*Gassum Fm* The porosity reduction is highest for very fine-grained sandstones and less for coarser-grained sandstones With respect to permeability, grain size has less influence than at shallow depths. Increasing grain size still leads to higher permeabilities, however
Detrital clay	*Bunter Sandstone Fm* Presence of inter-granular clay and clay clasts reduce porosity, but not substantially since much microporosity is present within the clays. Even small amounts of inter-granular clay reduce permeability considerably, whereas larger amounts of clay clasts are needed to produce a similar reduction in permeability *Gassum Fm* Presence of inter-granular clay and clay clasts reduce porosity. Detrital clays and/or clay clasts are often present. Clays and clay laminae lower the permeability, since some of the pore throats are very narrow	*Gassum Fm* The amount of clay increases with depth, but it has only minor effect on porosity, since the clay grows on the expense of other minerals. In addition, clay clasts increase the effect of compaction High amounts of detrital clays result in reduced permeability
Cement	*Bunter Sandstone Fm* Pervasive carbonate, anhydrite or halite cement may reduce porosity significantly, whereas patchy carbonate cement does not have a notable effect on porosity. Pervasive carbonate, anhydrite or halite cement occludes pores and thus prevents fluid flow. However, most commonly the cement is patchy and has only limited effect on fluid flow *Gassum Fm* Siderite and calcite cement occasionally result in larger porosity reduction than mechanical compaction. Presence of siderite cement leads to a marked reduction in permeability	*Gassum Fm* Pronounced porosity reduction with depth due to the presence of quartz and/or ankerite cement The permeability is markedly reduced where authigenic illite is present. Kaolinite has limited reducing effect on permeability. The permeability is primarily reduced by quartz and ankerite cement
Coatings	*Bunter Sandstone Fm* Sandstones with thick iron-oxide/hydroxide coatings are characterized by high permeability. The coatings may also preserve porosity *Gassum Fm* Sandstones with chlorite coatings have high permeability, unless other cement types are present	*Gassum Fm* Chlorite coatings may preserve porosity and permeability

Overall, the porosity distribution depends on the depositional environment and the maximum burial depth. Similarly, the permeability is strongly related to the depositional environment, which controls the distribution of grain sizes, the abundance of detrital clays, and the amount/type of cementing minerals etc. Based on information from Olivarius et al. (2015a) and Weibel et al. (submitted)

Our method for permeability prediction is based on averaging core and log data in order to derive average values for potential reservoir layers. The basic data for developing the 5-step procedure are Danish data as described below.

Well-log data, core analyses and well test data

Well-log data of variable quality have been acquired in hydrocarbon and geothermal exploration wells drilled in the Danish onshore area during the last *c.* 60 years. The porosity variation is determined from the interpretation of well-log data, and log interpretation results form the basis for calculating net sand properties. Both the total and the effective porosity of the reservoir units are considered. The total porosity (PHIT) is the total volume of inter-granular porosity plus clay bound water, whereas the effective porosity (PHIE) does not include the water bound by the clay particles. The core porosity data are directly comparable to the log-derived total porosity data. The term 'net sand' or 'potential reservoir layer' is herein defined as sandstone having minimum 15 % porosity and a clay or shale content of less than 30 %. These cut-offs are adopted from hydrocarbon exploration practice and applied herein to ensure that only potential reservoir sands with sufficient storage capacity and permeability are considered. Data representing non-reservoir sandstone and mudstone intervals are thus removed prior to further data analysis.

Only a limited number of well test data are available for permeability assessments in the Danish area, since most of the data for this study originates from dry hydrocarbon exploration wells. These wells were not tested, but usually logged and sometimes also cored. Accordingly, the present study focuses on alternative ways of predicting permeability, namely a combined analysis of petrophysical well-log data and routine permeability measurements on core plugs, with the objective to provide an average gas permeability of a particular reservoir unit. For that reason a direct link between the gas permeability measured in the laboratory and the actual liquid permeability of the reservoir in the subsurface is needed for precise pre-drilling estimates of the expected performance of a given geothermal reservoir.

All available core analysis data from the Danish onshore area have been considered in order to construct a robust database of porosity and permeability data. In general, measurements were performed according to the API RP-40 standard (American Petroleum Institute), i.e. He-porosity was measured at unconfined conditions and gas permeability was measured at a confining pressure of *c.* 2.8 MPa (400 psi), and at a mean nitrogen gas pressure of *c.* 0.15 MPa (*c.* 1.5 bar absolute). It is not always possible to obtain information about the test conditions, as the large number of analyses were performed over several decades and by various companies. These companies were, however, expected to follow the existing standards and it is thus assumed that measurements were conducted at conditions corresponding or comparable to the API RP-40 standard. Both Klinkenberg corrected and uncorrected gas permeabilities are included in the database, but primarily uncorrected permeabilities form part of the porosity–permeability plots presented herein.

Gas permeabilities measured in the laboratory do not equal reservoir permeabilities, whereas well test data are considered to provide reservoir permeability estimates on the condition that the height (thickness) of the test interval is well-known. Strictly speaking well test data only supply a transmissivity measure (i.e. reservoir height multiplied by reservoir permeability). Permeability interpreted from well test data is commonly up to 2 times higher than the corresponding core permeability (e.g. Wolfgramm et al. 2008); for example presence of fractures in the reservoir rock usually results in permeability enhancement. The presence of fractures or overall inhomogeneities cannot be validated for geothermal reservoir rocks onshore Denmark, but our interpretations of well test data from 5 wells indicate a liquid permeability that is about 1.5 times higher than the core permeability (Fig. 3). A prerequisite is that both core and well test permeabilities exist for the same interval.

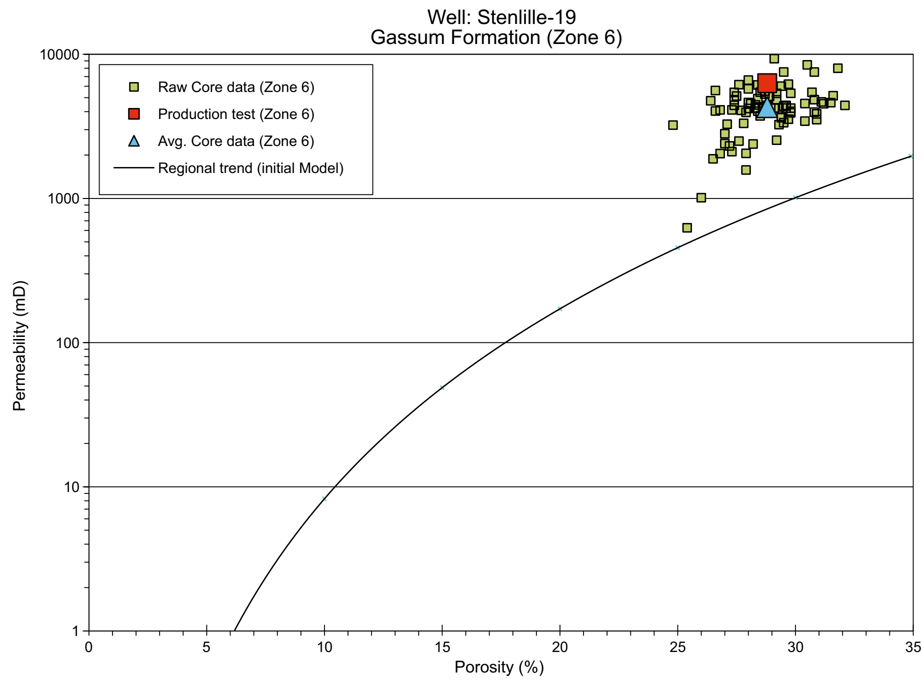

Fig. 3 Porosity–permeability plot, including a comparison between permeabilities derived from cores and well test data. Both unprocessed and averaged core permeability measurements are shown along with a reservoir permeability value linked to a production test conducted in the Stenlille-19 well (for location, see Fig. 1). The average core permeability (gas permeability) is about 4300 mD, whereas the well test permeability (liquid permeability) is about 6300 mD. Data originate from an excellent sandstone reservoir in the lower part of the Gassum formation (zone 6)

Prediction of porosity

First step in the 5-step procedure is to establish a porosity-depth model. The basic principle behind the porosity model is an assumed porosity-depth relationship, which previously has been documented for other basins (e.g. Gluyas and Cade 1997).

The porosity-depth model (step 1)

Seismic data provide information about depth and thickness of a geothermal prospect, but usually information about the average porosity must be modelled using porosity data from nearby wells. Porosities have primarily been interpreted from well-log data, and these data form the basis of establishing a correspondence between porosity and depth. The interpreted porosity log for each well is therefore averaged in order to determine the average porosity for specific reservoir intervals. A reservoir interval presumes a minimum porosity (herein >15 %) and a maximum shale content (herein <30 %) as described above. Therefore cut-offs were applied prior to calculating average porosities, i.e. the calculated porosities are average net porosities. The effect of applying cut-offs is that reservoir layers within each formation are identified and then assigned a porosity value on a well-to-well basis. One porosity-depth trend is observed for the Bunter Sandstone formation and another for the Gassum formation (Figs. 4, 5). The depth scale has been modified due to differential uplift across the Norwegian-Danish Basin (Japsen

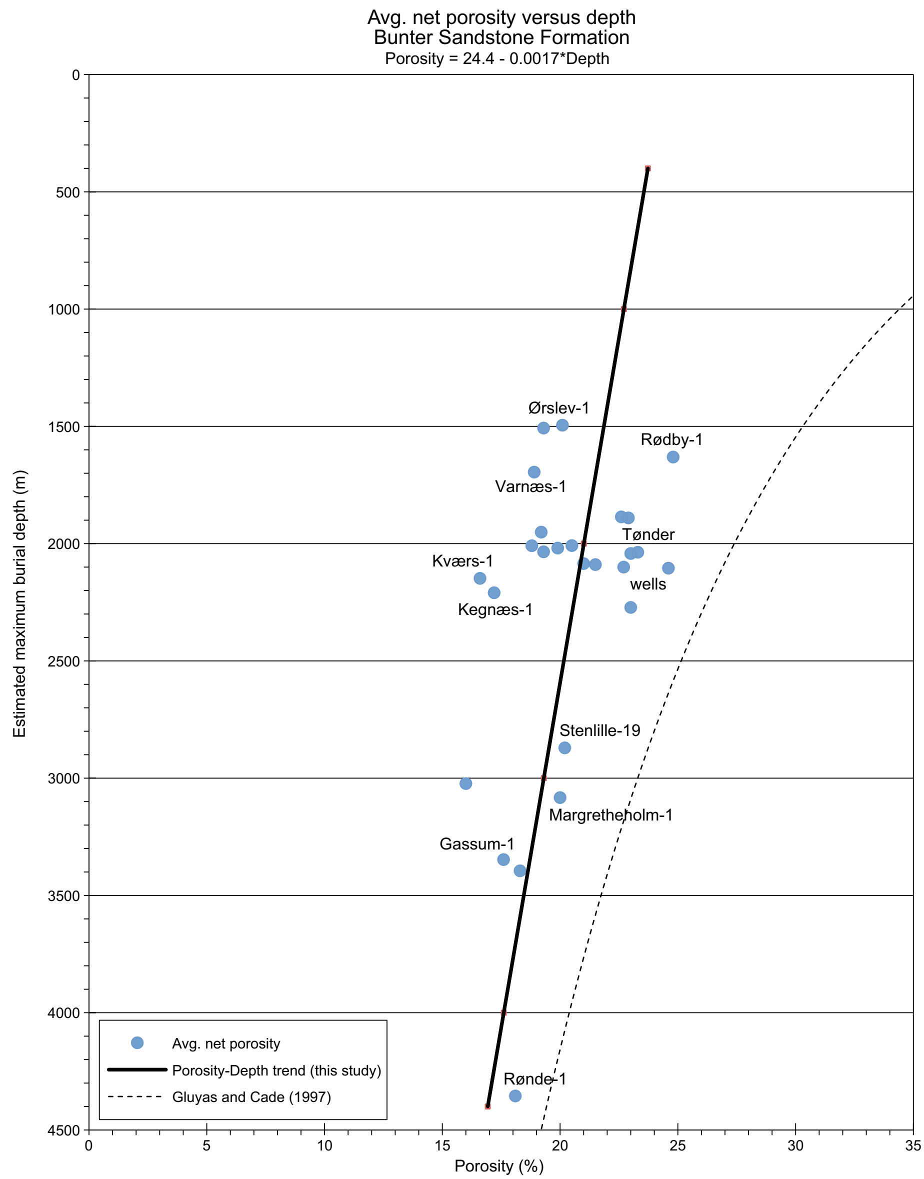

Fig. 4 Porosity model for the Bunter Sandstone formation. A porosity–depth relationship is suggested using data from selected Danish onshore and offshore wells. For well locations, see Fig. 1. The *depth scale* shows estimated maximum burial depth, as present-day depths have been corrected for differential uplift. The porosity is interpreted from well-log data (effective porosity). The average net porosity is calculated using cut-offs (min 15 % porosity; max 30 % shale). A mechanical compaction curve, i.e. a porosity–depth curve for *uncemented* sandstones published by Gluyas and Cade (1997), is shown for comparison (*dashed line*)

and Bidstrup 1999; Japsen et al. 2007), and hence the standard depth scale is replaced by 'estimated maximum burial depth'.

Prediction of permeability

In step 2–4 of the 5-step procedure a regional porosity–permeability model is established (step 2), refined (step 3) and adapted to be applicable to local conditions (step 4). Step 5 suggests a method to narrow the permeability uncertainty range.

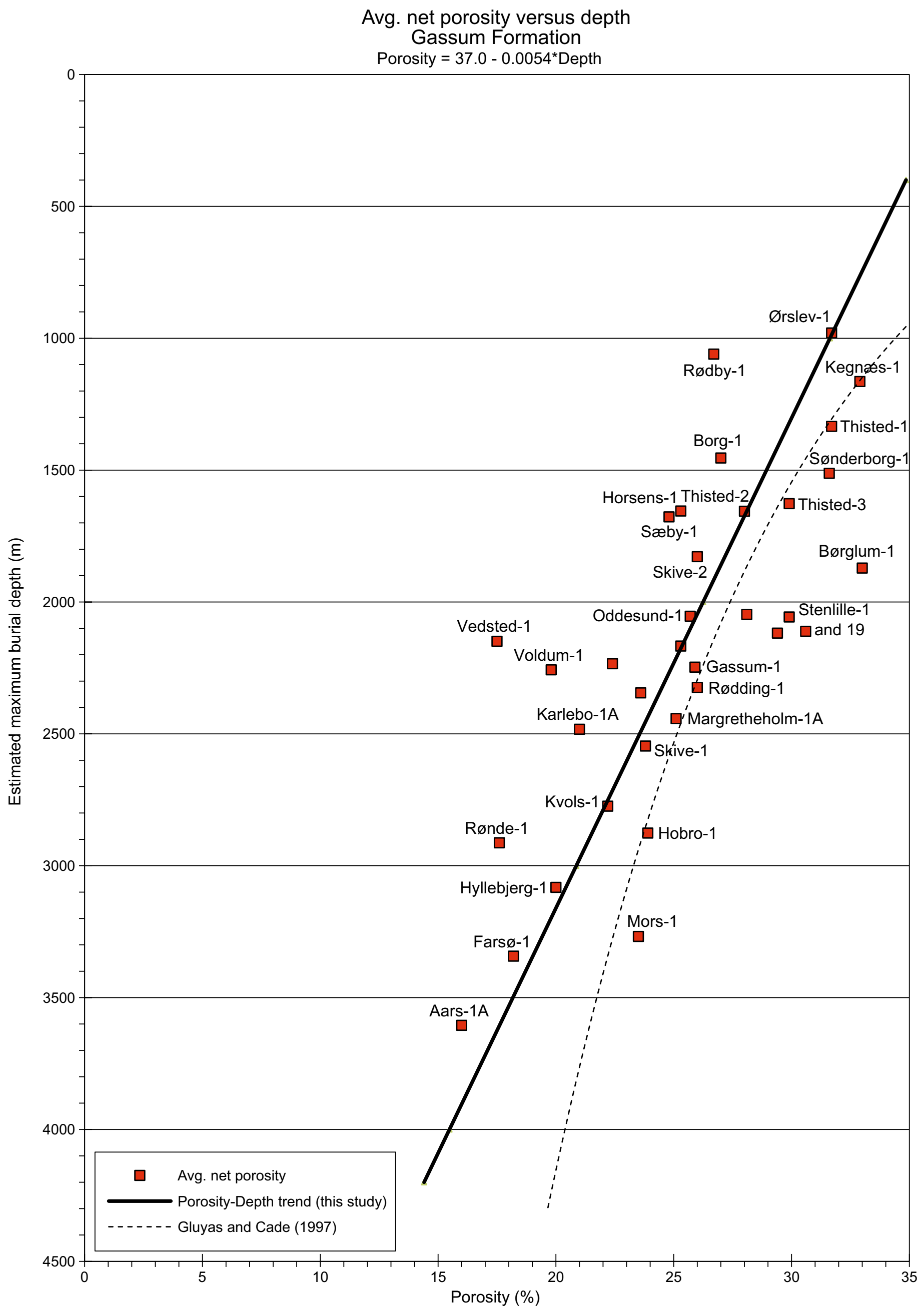

Fig. 5 Porosity model for the Gassum formation. A porosity–depth relationship is suggested using data from selected Danish onshore wells. For location of wells, see Fig. 1. The *depth scale* shows estimated maximum burial depth, as present-day depths have been corrected for differential uplift. The porosity is interpreted from well-log data (effective porosity). The average net porosity is calculated using cut-offs (min 15 % porosity; max 30 % shale). The porosity deterioration with depth is similar to the general trend in the majority of the onshore wells (Farsø-1, Horsens-1, Hyllebjerg-1, Kvols-1, Oddesund-1, Rødding-1, Skrive-1, Skive-2 and Ørslev-1. A mechanical (or normal) compaction curve published by Gluyas and Cade (1997) is shown for comparison

The initial permeability model (step 2)

Initially an empirical porosity–permeability relationship is established for each geological formation on the basis of available conventional core analysis data from all relevant wells using power-law-based curve fitting in line with the Kozeny law (Kozeny 1927). The resulting function used for calculating permeabilities is termed the initial permeability model and is illustrated in Fig. 6 and expressed in Eq. 1;

$$k_{\mathrm{ini}} = 3.47 \cdot 10^{-4} \cdot \varphi^{4.38}, \tag{1}$$

where k_{ini} is the initial permeability (in mD) and φ is the porosity (in %). The log-derived porosity was used as input data, and in this way a synthetic permeability log is assigned to all study wells, including the uncored wells. The permeability was calculated both from the effective and the total porosity, but the permeability curve calculated from the effective porosity is considered the most reliable permeability estimate, since it takes into account that the actual reservoir permeability is reduced in shaly and clayey intervals. However, the total porosity approximates the effective porosity in clean or almost shale-free reservoir intervals, and the synthetic permeability curves calculated from the total and effective porosity, respectively, are not significantly different in reservoirs with (very) low clay content.

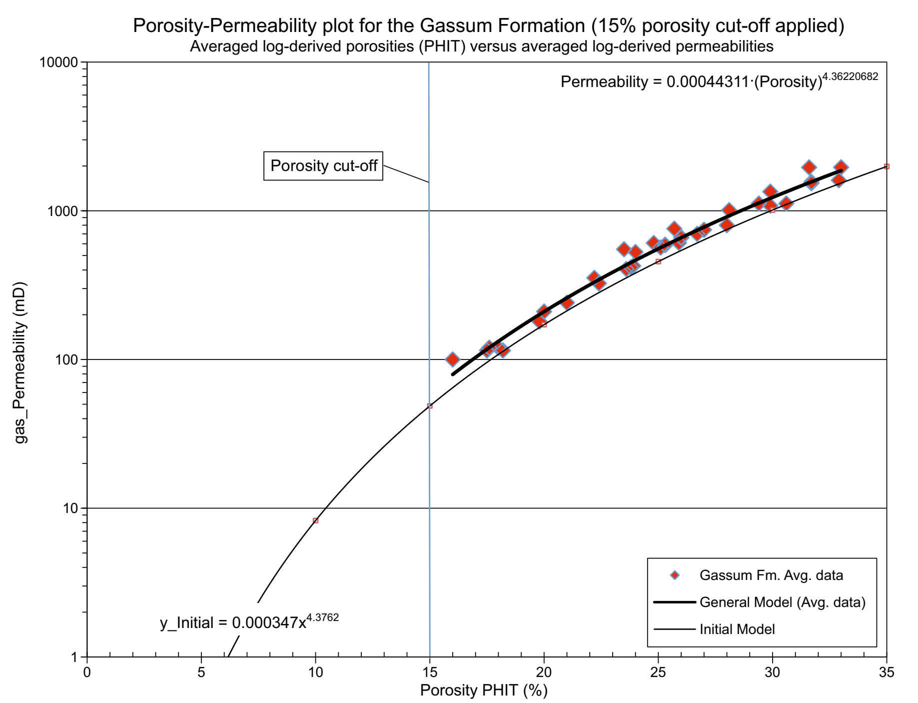

Fig. 6 Initial and general permeability model. Averaged log-derived porosity is plotted versus averaged log-derived permeability for a number of Danish onshore wells penetrating the Gassum formation, with the scope of setting up of a general permeability model (*bold line*). Each symbol (*diamond*) represents an average porosity and permeability value assigned to a particular well. The calculation of the averages is also based on two cut-off criteria: 15 % porosity cut-off and 30 % shale cut-off. Log-derived total porosity (PHIT) originates from interpretation of well-log data. Log-derived permeability is based on the log-porosity combined with the use of an empirical porosity–permeability relationship. The latter relationship corresponds to the initial model that is based on core analysis data only. Note that the averaging leads to an upward shift of the curve established prior to averaging. Permeability estimates based on the general model (*bold line*) are therefore somewhat higher than permeability estimates obtained from the initial model (*thin line*)

The general permeability model (step 3)

The next step is to average both the log-derived porosity curve and the log-derived permeability curve for the reservoir interval within each formation. Prior to this, shale and porosity cut-offs are applied in order to exclude non-reservoir data originating from clayey and cemented sections. These data do not contribute to the reservoir performance, but would otherwise influence the calculation of the average permeability if included. We assume a basinal setting with horizontal layering where the fluid flow is parallel to layer boundaries. In our opinion such a flow regime together with the cut-offs justify the use of arithmetic average for the operation.

A cross-plot between averaged porosity and permeability data points forms the basis of defining a new porosity–permeability relationship, the general permeability model, (Fig. 6) represented in Eq. 2:

$$k_G = 4.43 \cdot 10^{-4} \cdot \varphi^{4.36}, \tag{2}$$

where k_G is the general permeability (mD), and φ is the porosity (%). The porosity determined from the porosity-depth model (step 1) is used as input data for permeability modelling. Equation 2 is considered to be more representative of the full reservoir sections (Fig. 6; bold line). The calculated values are based on well-log data covering the reservoir section, and not only the cored parts of the formation. The introduction of the general permeability model also means that a specific permeability estimate becomes slightly higher than that calculated from the initial permeability model. The few available field test measurements confirm this observation.

The local permeability model (step 4)

The general permeability model represents the entire Danish onshore area and constitutes a template for constructing more refined local permeability models. Reservoir intervals of a specific formation in a local region may be characterized by deviating permeability distributions compared to the general trend (step 3). If local core permeability data are available, such data should therefore be used to calibrate the general permeability model to the local area. The use of the general permeability model in constructing local models is implemented with Eq. 3:

$$k_L = C \cdot k_G, \tag{3}$$

where k_L is the local permeability (in mD) and C is a constant controlled by the local permeability variations, and it may be determined from permeability measurements on core plugs from one or two local wells.

Core porosity and permeability data from selected wells drilled throughout the Danish onshore area have been averaged for each well and then compared to the general trend line (Fig. 7). The figure focuses on deviations from the general model, and it appears from the figure that permeability averages deviate by a factor of up to four as indicated by the upper and lower bounds, even though some data points fit the trend line. However, this spread is caused by the use of regional data representing the entire Danish onshore area, which masks local and often more limited permeability variations. The uncertainty connected to a local dataset is less than indicated by the regional data

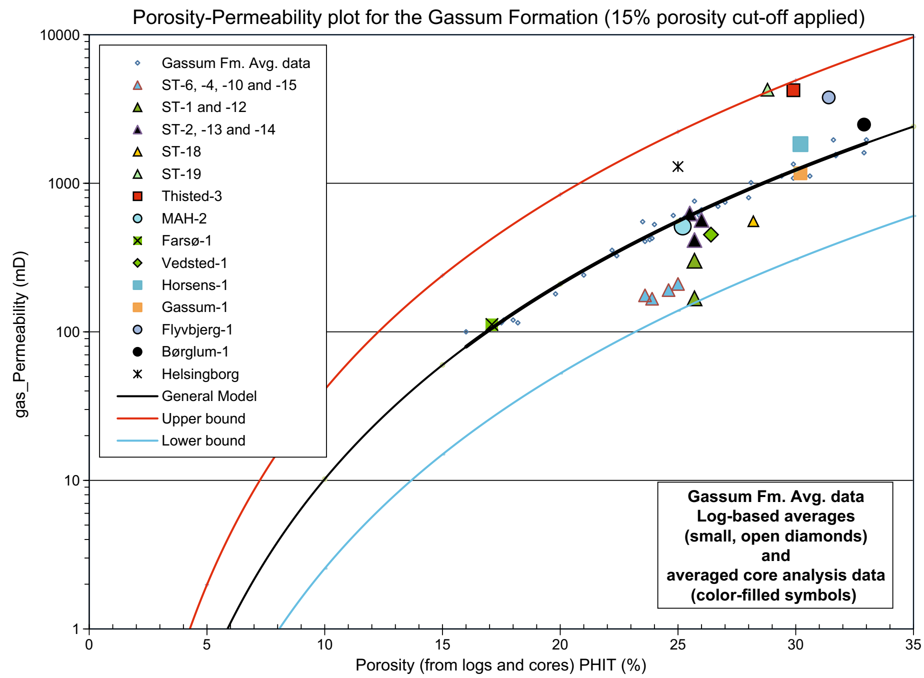

Fig. 7 Averaged core porosity data plotted versus averaged core permeability data for selected wells drilled throughout the Danish onshore area and that also have been cored in the Gassum formation (large, *colour-filled symbols*). A porosity cut-off of 15 % was applied prior to calculating averages. The general permeability model is shown as a *black solid line*; cf. Figure 6. The log-based averages used for defining the general permeability model are *plotted* with *small*, *open diamonds* and are added for comparison. The *upper* and *lower* bounds are *plotted* by *red* and *blue lines*, respectively. Observe that the log-based data do not form part of the core analysis database. *ST* Stenlille, *MAH* margretheholm, *PHIT* total porosity

set due to e.g. facies uniformity, and local permeability models are therefore needed for delivering locally adjusted permeability predictions.

Permeability uncertainty range (step5)

Even a local, calibrated porosity–permeability model is associated with an uncertainty range owing to the variations in lithology and diagenetic alterations within a limited local region (geological province). Such a restricted area may only be represented by one or two wells with wireline logs and no cores, and therefore it is difficult to determine a suitable uncertainty range related to the permeability estimate representative of any local area on the basis of such a limited database. In order to get an impression of the local variability, a selected area with good well coverage has been studied in detail. 20 wells have been drilled within a restricted area at the Stenlille gas storage facility located in the eastern part of the Norwegian-Danish Basin (Fig. 1), and a large database comprising both core analysis data and well-logs exists (these data are all available from the GEUS archives). Ten of these wells are cored in the upper part of the Gassum formation, and evaluation of 3D seismic data, correlation of well-logs and interpretation of cores indicate that relatively uniform geological conditions prevailed in the area during deposition. When all unprocessed core porosity and core permeability data representing the upper part of the Gassum formation are plotted in one cross-plot, the data points show an expected substantial scattering (Fig. 8). Hence the *averaged* core porosity and core permeability data are used to establish a local Stenlille model for this part of the Gassum formation and most importantly, also to assess the uncertainty range of the local porosity–permeability relationship (Fig. 9). The figure shows that the scatter is notably reduced when applying the averaging technique, but also that the distribution is displaced towards lower average permeabilities compared to the general model. This displacement could be due to differences in grain size as discussed later. The key message from the figure is, however, that the high and low bounds of the uncertainty band are limited by factors of 2 and 0.5 of the model mid-line.

Results

Result of porosity modelling

The result of the porosity modelling is the establishment of two regional porosity-depth trends as presented in Figs. 4 and 5.

Result of permeability modelling

Applying the averaging technique for predicting permeability on the basis of core permeability data and well-log interpretations adds to the applicability of porosity–permeability relations. A "best practice" method is suggested for predicting the average permeability of a potential geothermal reservoir. The average permeability of a geothermal prospect is modelled (predicted) using the closest local permeability model, i.e. a permeability model valid for a nearby geological province. This permeability value along with estimated net sand thickness are considered the key factors, when assessing the geothermal potential of a particular prospect. From our experience, the geothermal resource is of economic value if the reservoir transmissivity is greater than 10

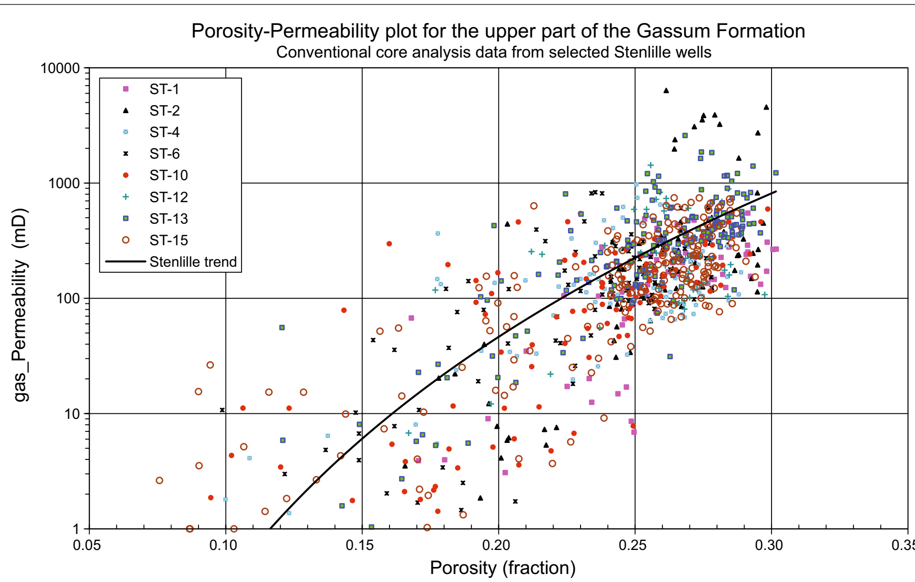

Fig. 8 *Plot* of core analysis data from a local field. The porosity–permeability *plot* is based on core samples from selected Stenlille gas storage facility wells. The data are measured on horizontally orientated plug samples. Data originate from the main reservoir section, i.e. the upper part of the Gassum formation. Note the *scattered data*. The Stenlille trend line (*black*) is calculated without applying any cut-offs. *ST* Stenlille

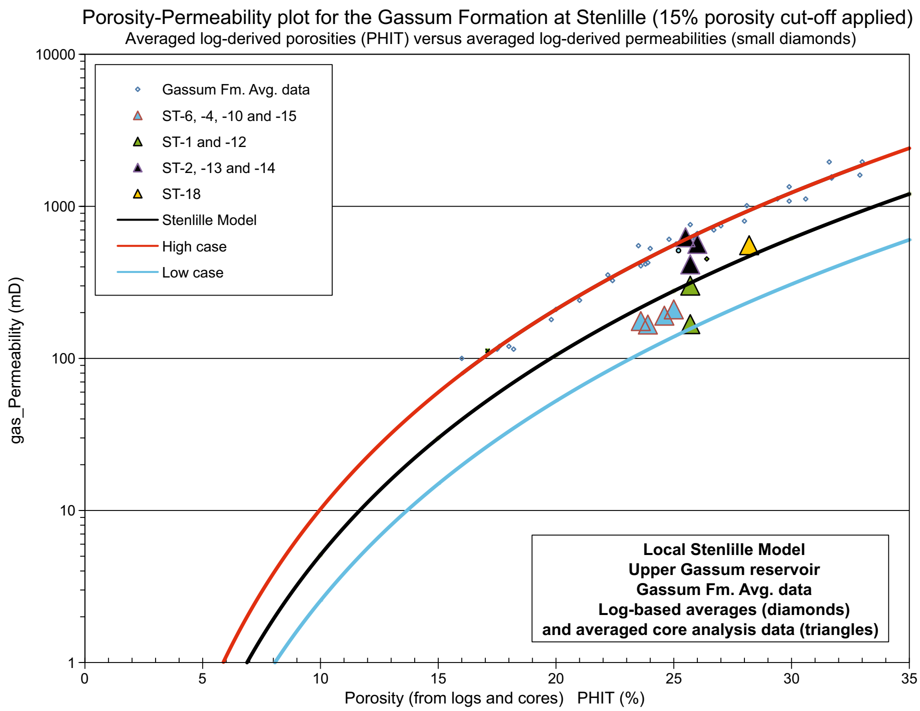

Fig. 9 Local Stenlille permeability model. The local model is shown by a *black solid line*. The uncertainty range is illustrated by a low case (*blue*) and a high case (*red*). The high and low bounds are limited by factors of 2 and 0.5 of the model mid-line (*black*). Averaged core porosity data are *plotted* versus averaged core permeability data for the 10 Stenlille wells cored in the upper part of the Gassum formation (*colour-filled symbols*). A porosity cut-off of 15 % was applied prior to calculating averages. Log-based averages used for defining the general permeability model are *plotted* for comparison (*small, open diamonds*). The local Stenlille permeability model is related to the general permeability through a constant (here $C = 0.5$); i.e. $k_L = 0.5 \cdot k_G$. The use of these factors (0.5 and 2) also implies that the high bound (*red*) equals the general permeability model in this particular case. *ST* Stenlille, *PHIT* total porosity

Darcy-metre. This assessment is in line with indicative values published in Seibt and Kellner (2003). The net sand thickness may be found from seismic isochores combined with extrapolation of net-to-gross ratios. Acquisition, interpretation and depth conversion of seismic data are thus pre-requisites for addressing the geothermal potential of a prospect. The determination of net sand thickness in a particular well is exemplified in Fig. 10.

Porosity–permeability plots based on conventional core analysis data are commonly scattered as shown and discussed above, but the use of the averaging technique presented herein reduces the scatter and narrows the width of the uncertainty band associated with a predicted average permeability value. It is thus recognized that the uncertainty of the average value is significantly smaller than the uncertainty of a single measurement.

Application of the methodology

The use of the methodology is exemplified by the derivation of a local model as presented in Fig. 11. The model is illustrated by mid-line, high and low bounds, defining an uncertainty envelope, and it is assumed that the model is a representative of the Gassum formation at the northern basin margin. Averaged core analysis data from wells located

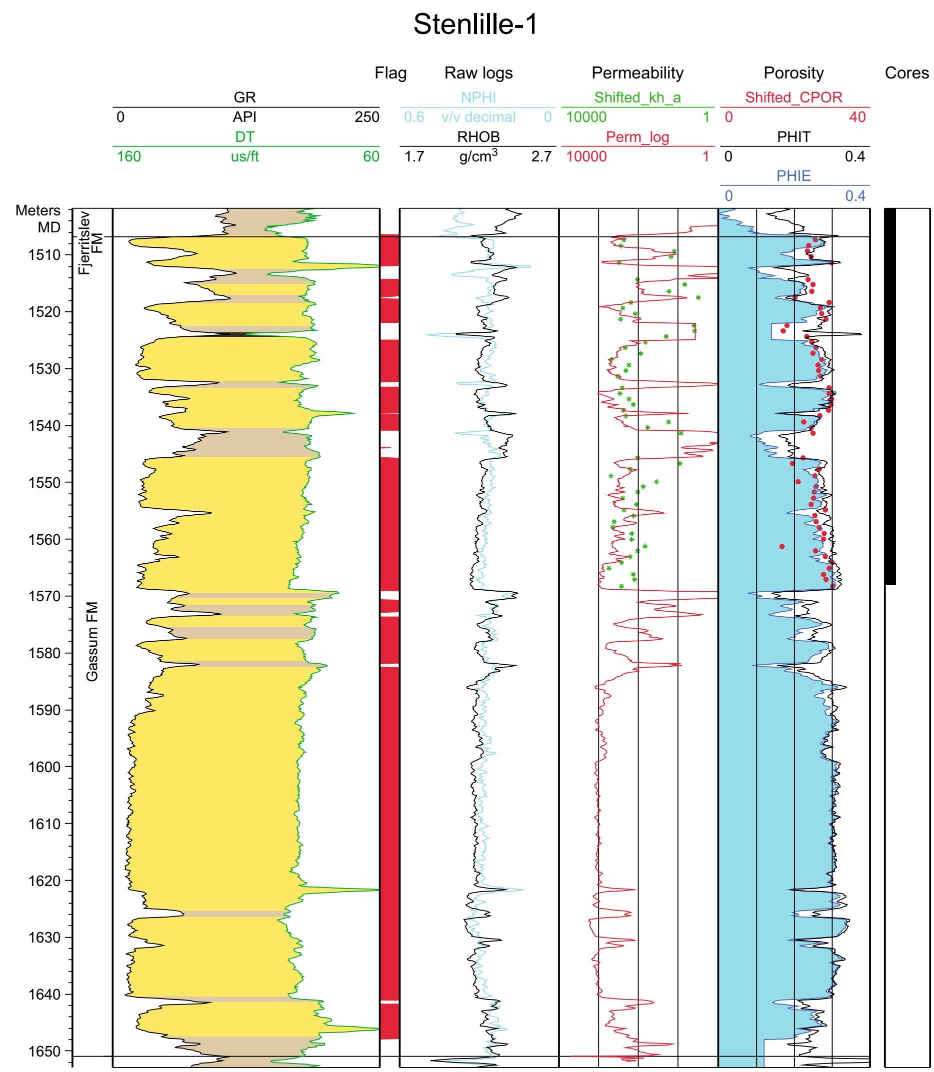

Fig. 10 Petrophysical evaluation of the Gassum formation in the Stenlille-1 well. The upper part of the formation is cored (*black bar*). The *red bar* indicates the location of potential reservoir layers (*net sand*) within the Gassum formation. Lithological interpretation; sandstone (*yellow*), shale (*brown*) and coal (*black*). Raw logs, *GR* gamma-ray log, *DT* sonic log, *RHOB* density log, *NPHI* neutron log. Interpreted logs; *PHIT* total porosity, *PHIE* effective porosity, *PERM_log* Synthetic permeability log. Core data; *CPOR* core porosity, *Kh_a* Core permeability. The PHIT and PHIE curves are interpreted from the well-log data, whereas the PERM_log curve is a calculated curve based on the local Stenlille permeability model. The core data are plotted as point data, showing a good match between the core porosity data and the log-derived porosity curve. Similarly, a reasonably good match is observed between core permeabilities and the synthetic, log-based permeability curve

in this area (Børglum-1 and Flyvbjerg-1; Fig. 1) point to permeabilities higher than indicated by the general model. A local model based on Eq. 3 was therefore established with the scope of predicting the average permeability of the Gassum formation in the Børglum–Flyvbjerg areas, expressed by Eq. 4:

$$k_{\mathrm{L}} = 1.7 \cdot k_{\mathrm{G}}, \tag{4}$$

where k_{L} is the local permeability (in mD) and the constant ($C = 1.7$) is determined from analysis of local core analysis data.

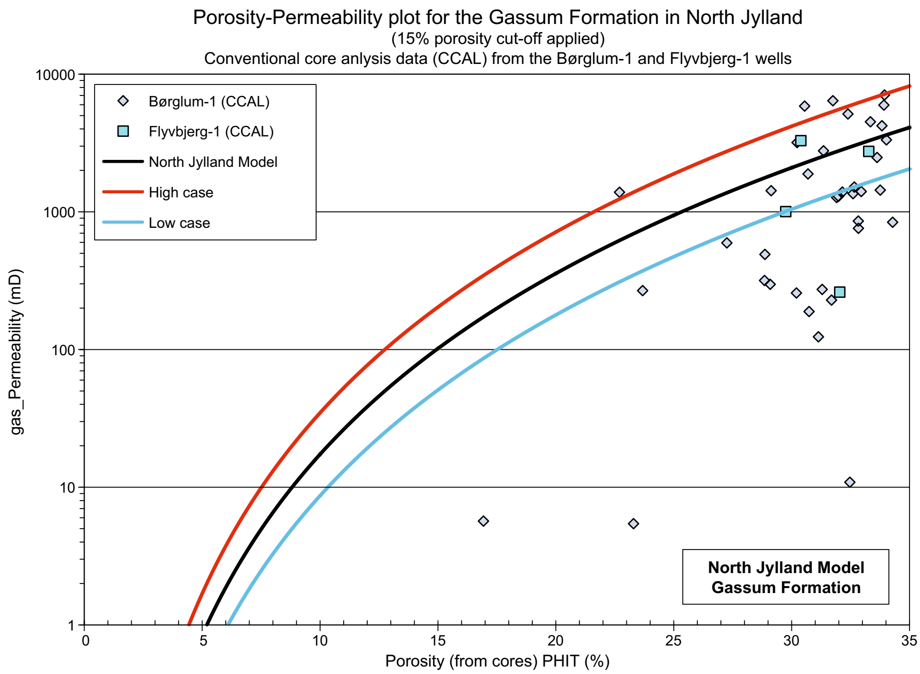

Fig. 11 Local permeability model representing the Gassum formation in North Jylland. The local area corresponds to the northernmost part of Denmark. The model is shown by a Mid-line (*black*), and the uncertainty range is illustrated by a Low case (*blue*) and a High case (*red*). The model is based on averaged core analysis data from the Børglum-1 and Flyvbjerg-1 wells (not shown) and the uncertainty range is related to the expected average permeability (indicated by *blue* and *red lines*). Conventional core porosity data are *plotted* versus core permeability data for the Børglum-1 and Flyvbjerg-1 wells cored in the Gassum formation (*colour-filled symbols*). The shale points, i.e. the data points plotting below the *blue line*, are not included in calculating averages. A porosity cut-off of 15 % was applied prior to plotting data. The uncertainty range is connected to the expected average permeability and thus it is not connected to the dataset consisting of conventional core analysis data. The local North Jylland permeability model is related to the general permeability model through a constant; i.e. Local North Jylland permeability model = 1.7 × general permeability model

The conventional core analysis data from the Børglum-1 and Flyvbjerg-1 wells are also plotted after applying a porosity cut-off (Fig. 11). The mid-line honours calculated averages of the core analysis data from the two wells. Data points plotting below the uncertainty envelope were, however, excluded prior to calculating averages, because these data points represent sandstones with large amounts of fine-grained material (shale, mudstone and siltstone) not contributing to reservoir performance. The width of the uncertainty band is transferred from our Stenlille study, i.e. factors of 2 and 0.5 define the high and low bounds. The uncertainty band does not address the spread in the actual core analysis data, but it points out an uncertainty range that is related to the average permeability for a typical reservoir, presuming that the reservoir sandstones are almost shale-free. Furthermore, the example demonstrates that it is difficult to narrow the uncertainty range on the basis of a limited set of conventional core analysis data.

Discussion

A number of porosity–permeability trends have been analysed to obtain a better understanding of the relationship between porosity and permeability. It is recognized that the porosity and permeability distribution is affected by burial depth and grain size (Table 1), but the influence of depositional environment, sediment source area, transport distance and diagenesis far from well control is not yet fully understood and is therefore difficult to quantify. Models for estimating porosities and permeabilities have, nevertheless, been established, but are associated with uncertainty.

Prediction of porosity

The formation brines of the potential reservoir sandstones in the Danish onshore area are characterized by hydrostatic pressure, so sandstone porosity is not affected by overpressure. Knowledge of the pressure distribution across the Danish onshore area comes from analysis of well test data. Our study indicates, however, that the sandstone porosity more likely is related to geological factors such as burial depth, lithofacies, clay content and diagenesis. In addition, the porosity-depth trend is affected by differential uplift and erosion; thus present-day depths were corrected for uplift using exhumation data presented in Japsen and Bidstrup (1999) and Japsen et al. (2007). For simple modelling purposes in undrilled areas, the porosity may be considered to be controlled by depth alone, provided that 'present-day depths' are replaced by 'estimated maximum burial depths'.

One porosity-depth trend is observed for the Bunter Sandstone formation and another for the Gassum formation (Figs. 4, 5), despite the fact that local deviations from the general trends are observed. These deviations are presumably related to geological factors as outlined above. An empirical porosity-depth relationship by Gluyas and Cade (1997) is also plotted to compare the current porosity-depth trends with a suggested normal compaction curve. The Gluyas and Cade curve presumes no uplift and reflects mechanical compaction in uncemented sandstones from hydrocarbon fields with high porosity and no overpressure. These general porosity-depth trends (cf. Figs. 4, 5) are suggested for predicting the average porosity of potential reservoir sandstones in undrilled areas. A complete match between depth and porosity has not been fully achieved although maximum burial depths are applied, since the porosity also depends on factors other than depth, e.g. gain size (Table 1). However, for modelling purposes the use of a porosity-depth relation is considered satisfactory for porosity prediction and assessment. Consequently, modelled porosities are associated with uncertainty, even if the reservoir depth is well-known prior to drilling. In specific areas where the porosity distribution is well-known from local well and core data (e.g. at Tønder; Fig. 1), a local porosity-depth trend should be used.

Porosity of the Bunter sandstone formation

Porosities of the Bunter sandstone formation are generally lower than derived from the mechanical compaction curve published by Gluyas and Cade (1997), indicating that most sandstones of the Bunter Sandstone formation contain clays and diagenetic cements (Fig. 4). The Bunter sandstone formation retains relatively high porosity at greater depths, as detrital clays contain microporosity and diagenetic iron-oxide/hydroxide coatings seem to retard quartz cementation (Table 1; Olivarius et al. 2015a). The Tønder area in the southernmost part of Denmark (Fig. 1) is a potential site for geothermal exploitation and here the Bunter Sandstone reservoir (situated at a depth of 1500–2000 m) is characterized by average porosities (*c.* 22 %) that are higher than indicated by the general trend line. The porosity development at Tønder is mainly due to a dominance of aeolian deposition that favoured generation of very well-sorted and clay-free sandstones, but also the presence of nitrogen gas contributes to porosity preservation during burial cf. the Tønder-3 and -4 well completion reports (Mærsk 1981; Dong 1983). The Kegnæs-1 and Kværs-1 wells, also located in the southern part of Denmark, have encountered the Bunter Sandstone formation at a similar depth (1500–2000 m), but here the porosities (*c.* 17 %) are somewhat lower than indicated by the general trend for the Bunter Sandstone formation. Cutting descriptions reported in the well completion reports (Mærsk 1985; Texaco 1985) indicate that this porosity difference most likely is attributed to the presence of more fine-grained sandstones with higher clay content at Kegnæs and Kværs.

Porosity of the Gassum formation

The porosities are generally higher for the Gassum formation than for the Bunter Sandstone formation when considering shallow depths (<*c.* 3000 m), but the reservoir intervals of the Gassum formation show a steeper porosity–depth gradient. The overall porosity deterioration with depth is about five porosity units (%) per 1000 m (Fig. 5), and this trend is presumably a result of mechanical compaction combined with the effect of diagenetic alterations (Table 1). As an example, the reservoir sandstones at the Stenlille gas storage facility are characterized by porosities (*c.* 30 %) that are higher than indicated by the general trend line (see Fig. 1 for location). This porosity development is probably due to dominance of well-sorted shoreface sandstones. A maximum burial depth of *c.* 2100 m is estimated for the Gassum formation at Stenlille, and the present-day depth of *c.* 1500 m is due to uplift. In most wells, the porosity deterioration with depth corresponds to the general trend irrespective of correction for uplift (Figs. 1, 4). In the Børglum-1 well, in contrast, the porosity of the reservoir interval is extraordinarily high (33 %) compared to burial depth, primarily due to the occurrence of unconsolidated sandstone layers in this interval. The reservoir intervals of the Gassum formation likewise exhibit porosities that locally are lower than modelled from the porosity-depth trend, presumably because of variations in diagenetic development (e.g. the Voldum-1 well in which the porosity is *c.* 18 %).

Prediction of permeability

Reservoir performance, including flow rates, is closely related to porosity and permeability, and information about permeability is essential for determining reservoir transmissivity unless well test data are available. Correct prediction of sandstone permeability is a challenge for potential geothermal reservoirs, since fluid flow depends on a number of factors. Compaction processes, precipitation of cement and presence of detrital clay lead to smaller pore throat sizes, thus lowering the resulting reservoir permeability.

Usually there is a relatively clear correlation between core porosity and core permeability data, but this correlation is somewhat ambiguous due to scattered data resulting from differences in the depositional environment, clay content and diagenetic development. The variability in the core analysis data means that a perfect correlation between core porosity and core permeability data cannot be obtained. Despite these uncertainties, this computed porosity–permeability relation forms the basis of calculating a log-based permeability curve for each well using the log-derived porosity as input data.

The observed variation in permeability for a fixed porosity value (Fig. 7) is most likely related to variations in the original depositional environment when the sandstone layers were formed, expressing itself in differences in diagenetic development, lithology, grain size distribution and clay content (Table 1). These variations emphasize the need of incorporating geological data, preferably both sedimentological and palaeogeographical data, and also the need for establishing local porosity–permeability models representative of local geological provinces characterized by relatively uniform geological development. Such local permeability models are herein suggested for predicting the average permeability of geothermal prospects. In fact, access to local permeability data from wells located close to the prospect in question is essential for using our method for predicting permeability.

In addition to the porosity-depth model, it could be relevant to set up a general, basin-wide permeability-depth model. However, such a model will be rather uncertain, because depth is not the single most important factor for assessing the permeability. Sandstone porosity and grain size are also responsible for permeability development (cf. the Kozeny law). It is, nevertheless, suggested to link permeability to depth in 2 steps:

1. Depth is converted into porosity using a porosity-depth model.
2. Porosity is converted into permeability using a porosity–permeability relationship defined by a local permeability model. A local permeability model accounts for differences in grain size and diagenetic development (Table 1). When combining these two items, the permeability of the Gassum formation may be expressed as function of depth (Eq. 5):

$$k_{\mathrm{L}} = C \cdot k_{\mathrm{G}} = C \cdot 4.43 \cdot 10^{-4} \cdot \varphi^{4.36} = C \cdot 4.43 \cdot 10^{-4} \cdot (37 - 0.0054 \cdot Z)^{4.36}, \qquad (5)$$

where k_{L} is the local permeability (mD), k_{G} is the general permeability (mD), C is a constant, φ is the porosity (%) and Z is the maximum burial depth (m). The porosity-depth equation for the Gassum formation (Fig. 5) is also applied. Inserting $C = 1$ in Eq. 5 will give an initial assessment of the permeable conditions at depth.

The methods presented herein are developed on the basis of data from Danish geothermal reservoirs. The methodology for predicting average porosity and permeability is, however, considered applicable to similar sandstone reservoirs in other settings, but it has to be proved with additional data.

Permeability uncertainty range based on local field data

The width of the uncertainty band related to average permeability is addressed by analysing core analysis data from the local Stenlille field with several cored and logged wells located closely together. A petrophysical evaluation of the Gassum formation in the Stenlille-1 well is illustrated in Fig. 10. The character of the Gassum formation at Stenlille is considered representative of geothermal reservoirs found in the formation onshore Denmark. The Gassum formation consists of a number of sandstone layers interbedded with clay-rich intervals. Hence the Gassum formation is assigned a lithology column along with porosity and permeability curves as shown in Fig. 10. The porosity is interpreted from well-log data, whereas the permeability is calculated from the porosity–permeability relationship shown in Fig. 8.

A local Stenlille permeability model was initially established on the basis of averaged core porosity and permeability data from 10 Stenlille wells cored in the upper part of the Gassum formation, corresponding to the main gas storage reservoir (Fig. 9). In addition, the core analysis data are relevant for calibrating the log-based porosity and permeability interpretations (Fig. 10). Less core material exists from the lower part of the Gassum formation and the geological conditions that prevailed during deposition of the lower part differ from those of the upper part (Nielsen et al. 1989; Nielsen 2003). With respect to permeability, the core analyses show that the overall Stenlille permeability is approximately a factor 2 less than the permeability estimated from the general, basin-scale model (Fig. 9). The lower average permeability values observed at Stenlille are presumably caused by dominance of finer-grained sandstone compared to the sandstones defining the general permeability model. The presence of fine-grained reservoir sandstones at Stenlille is evidenced by sedimentological core log descriptions of the Stenlille-1 core (Nielsen et al. 1989). The permeabilities of these sandstones (Fig. 8) are generally lower than commonly seen in Gassum formation sandstones deposited elsewhere, and the lower permeability level at Stenlille may therefore be linked to grain size.

The averaged core analysis data from the Stenlille wells suggest that the uncertainty range can be expressed by multipliers of 2 and 0.5 (Fig. 9). This procedure involves multiplying and dividing the local Stenlille permeability trend by a factor of 2 in order to determine an upper and lower bound that delineate the data points, i.e. an envelope ranging from the lowest to the highest average permeability values. As the core permeability data do not follow a normal distribution, the uncertainty cannot be described by conventional standard deviation and instead, we suggest applying this uncertainty envelope. We assume the Stenlille dataset to be relevant for assessing the uncertainty range for a typical Gassum geothermal reservoir at any location in Denmark.

Conclusions

The major outcome of this study is the development of a "Best practice" technique for predicting porosity and permeability in sandstone reservoirs located in areas with poor data coverage. A 5-step procedure has been developed for assessing porosity and permeability in the Danish area:

1. Establishing a regional porosity-depth model.
2. Establishing an initial permeability model based on a conventional porosity–permeability plot using core analysis data from all cored study wells.
3. Establishing a general permeability model where both porosity and permeability are replaced by averaged log-derived data.
4. Using the general permeability model as a template for establishing local permeability models.
5. Using the Stenlille model to describe the uncertainty range of a permeability estimate obtained from a local permeability model.

Furthermore, the following conclusions can be provided based on our present knowledge:

- Application of the 5-step technique using averaged porosity and permeability data significantly reduces the scattering of data points that is normally seen in conventional porosity–permeability plots. This observation is related to the fact that the uncertainty of an average value is significantly lower than the uncertainty of a single measurement.
- The available database is comprehensive and it comprises both widely and sporadically distributed data, meaning that a statistical approach to data analysis is not feasible. Instead an empirical approach has been used.
- The average porosity of a particular sandstone reservoir in a geothermal prospect is herein considered to be related primarily to depth. Models for porosity prediction are established for the Bunter sandstone and the Gassum formations.
- A permeability model that is based on averaging both log-derived porosities and permeabilities is introduced (general permeability model). The porosity determined from the porosity-depth model is used as input data for the permeability modelling.
- We consider local permeability models suitable for permeability prediction. Local permeability models account for variations in burial depth, grain size and diagenetic alterations.
- A permeability-depth modelling method is suggested. The permeability is, however, related to factors other than depth such as grain size, detrital clay content and diagenetic development, including presence of cement and authigenic clays (Table 1).
- We have compared permeabilities interpreted from well test data with core permeability measurements whenever possible (5 wells). Seemingly, core permeability data measured in the laboratory resemble the reservoir permeability, provided that an appropriate correction or upscaling factor is applied.
- The geothermal potential of a particular prospect should be assessed using modelled porosity and permeability values combined with thicknesses derived from seismic interpretations. Thus an assessment of the transmissivity is essential, and in this context modelled permeabilities and estimated net sand thicknesses are key input parameters.
- The uncertainty range related to the average permeability of a geothermal prospect is addressed using a comprehensive local field dataset from the Stenlille gas storage facility. Local field data are geographically and geologically constrained and therefore suitable for analysing a local uncertainty range connected to a specific site. Our data analysis suggests that the uncertainty range related to the average permeability can be expressed by multipliers of 2 and 0.5.

Authors' contributions

LK carried out the petrophysical evaluation, performed the data analysis, participated in the construction of the porosity–permeability models and drafted the manuscript. MLH participated in the log analyses and contributed considerably to the drafting of the manuscript. PF contributed to the development and design of the permeability prediction model. MO and RW performed the diagenetic investigations, dealing with the Bunter Sandstone formation (MO) and the Gassum formation (RW). LHN and AM participated in the design of the study and contributed to the regional interpretations of the results and to the drafting of the manuscript. All authors have read and commented early drafts and have approved the final manuscript. All authors read and approved the final manuscript.

Author details

[1] Geological Survey of Denmark and Greenland (GEUS), Øster Voldgade 10, 1350 Copenhagen, Denmark. [2] Department of Geoscience, Aarhus University, Høegh-Guldbergsgade 2, 8000 Aarhus, Denmark.

Acknowledgements
This paper is published with permission of the Geological Survey of Denmark and Greenland and is an outcome of the project "The geothermal energy potential in Denmark—reservoir properties, temperature distribution and models for utilization" under the "Sustainable Energy and Environment" programme founded by the Danish Council for Strategic Research. We would like to thank professor Kim Esbensen (GEUS) for valuable discussions and for constructive comments on the manuscript text. Stefan Sølberg (GEUS) improved the artwork considerably.

Competing interests
The authors declare that they have no competing interests.

Received: 1 November 2015 Accepted: 21 March 2016
Published online: 01 April 2016

References

Bachmann GH, Geluk MC, Warrington G, Becker-Roman A, Beutler G, Hagdorn H, Hounslow MW, Nitsch E, Röhling H-G, Simon T, Szulc A. Triassic. In: Doornenbal H, Stevenson A, editors. Petroleum geological atlas of the Southern Permian Basin area. Rotterdam: European Association of Geoscientists and Engineers Publications; 2010. p. 149–73.

Balling N, Kristensen JI, Breiner N, Poulsen KD, Rasmussen R, Saxov S. Geothermal measurements and subsurface temperature modelling in Denmark. GeoSkrifter. 1981;16:172.

Balling N, Poulsen SE, Bording TS, Fuchs S, Mathiesen A. Surface temperatures in Denmark—measurements and modelling. Abstract and poster presentation. Copenhagen: Energi-og miljøkonference; 2014.

Berthelsen F. Lithostratigraphy and depositional history of the Danish Triassic. Geological Survey of Denmark; 1980. Series B, No 4.

Block S. Empirical prediction of porosity and permeability in sandstones. Am Assoc Pet Geol Bull. 1991;75:1145–60.

Carman PC. Fluid flow through granular beds. Trans Inst Chem Eng. 1937;15:150–66.

Carman PC. Flow of gasses through porous media. London: Butterworth Scientific Publications; 1956.

Clausen OR, Pedersen PK. Late Triassic evolution of the southern margin of the Ringkøbing-Fyn High. Mar Pet Geol. 1999;16:653–65.

Clemmensen LB. Desert sand plain and sabkha deposits from the Bunter Sandstone formation (L. Triassic) at the northern margin of the German Basin. Geol Rundsch. 1985;74:519–36.

Dong. Tønder-4 gas exploration well. Well summary. Dansk Olie og Naturgas A/S; 1983.

Doyen PM. Permeability, conductivity and pore geometry of sandstone. J Geophys Res. 1988;93:7729–40.

Duan Q, Yang X. Experimental studies on gas and water permeability of fault rocks from the rupture of the 2008 Wenchuan earthquake, China. Sci China Earth Sci. 2014;57(11):2825–34.

Ehrenberg SN. Relationship between diagenesis and reservoir quality in sandstones of the Garn formation, Haltenbanken, Mid-Norway Continental Shelf. Am Assoc Pet Geol Bull. 1990;74:1538–58.

Evans J, Cade C, Bryant S. A geological approach to permeability prediction in clastic reservoirs. In: Kupecz JA, Gluyas J, Block S, editors. Reservoir quality prediction in sandstones and carbonates AAPG Memoir 69; 1997. p. 91–101.

Gluyas J, Cade CA. Prediction of porosity in compacted sands. In: Kupecz JA, Gluyas J, Block S, editors. Reservoir quality prediction in sandstones and carbonates. AAPG Memoir 69; 1997. p. 19–28.

Hjuler ML, Erlström M, Lindström S, Nielsen LH, Kristensen L, Mathiesen A, Bidstrup T. Extended evaluation of possible geothermal reservoirs in the Helsingør area including geological data from Helsingborg and Øresund. Contribution to an evaluation of the geothermal potential. Geological Survey of Denmark and Greenland Report 2014/29; 2014.

Japsen P, Bidstrup T. Quantification of late Cenozoic erosion in Denmark based on sonic data and basin modelling. Bull Geol Soc Den. 1999;46:79–99.

Japsen P, Green PF, Nielsen LH, Rasmussen ES, Bidstrup T. Mesozoic-Cenozoic exhumation events in the eastern North Sea Basin: a multi-disciplinary study based on palaeothermal, palaeoburial, stratigraphic and seismic data. Basin Res. 2007;19:451–90.

Kazemi A, Shaikhina D, Pickup G, Corbett P. Comparison of upscaling methods in a heterogeneous carbonate model. SPE 154499. EAGE Annual Conference and Exhibition, Copenhagen, June 4–7; 2012.

Kirsch R, Balling N, Fuchs S, Hese F, Hjuler ML, Kristensen L, Mathiesen A, Nielsen CM, Nielsen LH, Offermann P, Poulsen NE, Rabbel W. GeoPower: Varme fra undergrunden til Sønderjylland–Schleswig–Erdwärme für die Region Südjütland–Schleswig. Technical Report. Schriftenreihe: LLUR SH–Geologie und Boden; 21. Landesamt für Landwirtschaft, Umwelt und ländliche Räume des Schleswig-Holstein; 2015.

Klinkenberg LJ. The permeability of porous media to liquids and gases, drilling and production practice, American Petroleum Inst.; 1941. p. 200–13.

Kozeny J. Über kapillare Leitung des Wassers im Boden. Akademi der Wissenschaften in Wein, Sitzungsberichte, Abt. 2a, 136; 1927. p. 271–306.

Lott GK, Wong TE, Dusar M, Andsbjerg J, Mönning E, Feldman-Olszewska A, Verreussel RMCH. Jurassic. In: Doornenbal H, Stevenson A, editors. Petroleum geological atlas of the Southern Permian Basin area. Rotterdam: European Association of Geoscientists and Engineers Publications; 2010. p. 175–93.

Mathiesen A, Kristensen, L, Bidstrup T, Nielsen LH. Vurdering af det geotermiske potentiale i Danmark. Geological Survey of Denmark and Greenland Report 2009/59; 2009.

Mathiesen A, Kristensen, L, Bidstrup T, Nielsen LH. Evaluation of possible geothermal reservoirs in the Tønder area. Contribution to an evaluation of the geothermal potential. Geological survey of Denmark and Greenland Report 2010/90 (confidential); 2010a.

Mathiesen A, Nielsen LH, Bidstrup T. Identifying potential geothermal reservoirs in Denmark. Geol Surv Denmark Greenland Bull. 2010;20:19–22.

Mathiesen A, Kristensen, L, Nielsen CM, Weibel R, Hjuler ML, Røgen B, Mahler A, Nielsen LH. Assessment of sedimentary geothermal aquifer parameters in Denmark with focus on transmissivity. In: Proceedings European geothermal congress 2013. Pisa; 2013.
Mavko G, Nur A. The effect of a percolation threshold in the Kozeny-Carman relation. Society of exploration geophysicists. Geophysics. 1997;62:1480–2.
Michelsen O, Nielsen LH. Structural development of the Fennoscandian Border Zone, offshore Denmark. Mar Pet Geol. 1993;10:124–34.
Michelsen O, Clausen OR. Detailed stratigraphic subdivision and regional correlation of the southern Danish Triassic succession. Mar Pet Geol. 2002;19:563–87.
Michelsen O, Nielsen LH, Johannessen P, Andsbjerg J, Surlyk F. Jurassic lithostratigraphy and stratigraphic development onshore and offshore Denmark. In: Ineson JR, Surlyk F, editors. The Jurassic of Denmark and Greenland. Geological Survey of Denmark and Greenland Bulletin 1; 2003. p. 147–216.
Mærsk. Tønder-3 Completion Report. Dansk Boreselskab A/S; 1981.
Mærsk. Kværs-1 Completion Report. Mærks Olie og Gas A/S; 1985.
Nielsen LH, Larsen F, Frandsen N. Upper Triassic–Lower Jurassic tidal deposits of the Gassum formation on Sjælland, Denmark. Geological Survey of Denmark; 1989. Series A, No 23.
Nielsen LH, Japsen P. Deep wells in Denmark 1931–1990. Lithostratigraphic subdivision. Geological Survey of Denmark. DGU; 1991. Series A, No. 31.
Nielsen LH. Late Triassic–Jurassic development of the Danish Basin and Fennoscandian Border Zone, Southern Scandinavia. In: Ineson JR, Surlyk F, editors. The Jurassic of Denmark and Greenland. Geological Survey of Denmark and Greenland Bulletin 1; 2003. p. 459–526.
Nielsen LH, Mathiesen A, Bidstrup T. Geothermal energy in Denmark. Review of survey activities 2003. Geol Surv Denmark Greenl Bull. 2004;4:17–20.
Norden B, editor. Geothermal energy utilization in low-enthalpy sedimentary environments. Scientific Technical Report 11/06. German Research Centre for Geosciences (GFZ), Potsdam; 2011.
Olivarius M, Weibel R, Hjuler ML, Kristensen L, Mathiesen A, Nielsen LH, Kjøller C. Diagenetic effects on porosity–permeability relationships in red beds of the Lower Triassic Bunter Sandstone formation in the North German Basin. Sed Geol. 2015a;321:139–53.
Olivarius M, Weibel R, Friis H, Boldreel LO, Keulen N, Thomsen TB. Provenance of the Lower Triassic Bunter Sandstone formation: implications for distribution and architecture of aeolian vs. fluvial reservoirs in the North German Basin. Basin Res. 2015b. doi:10.1111/bre.12140.
Olivarius M, Nielsen LH. Triassic paleogeography of the greater eastern Norwegian-Danish Basin: constrains from provenance analysis of the Skagerrak formation. Mar Pet Geol. 2016;69:168–82.
Pharaoh TC, Dusar M, Geluk MC, Kochel F, Krawezyk C, Krzywiec P, Schech-Wenderoth M, Thybo H, Vejbæk O, Diederik van Wees J. Tectonic evolution. In: Doornenbal H, Stevenson A, editors. Petroleum geological atlas of the Southern Permian Basin area. Rotterdam: European Association of Geoscientists and Engineers Publications; 2010. p. 25–57.
Poulsen SE, Balling N, Bording TS, Mathiesen, A, Nielsen SB (submitted) Regional-scale subsurface temperature modelling with inverse methodology: application to Danish sedimentary basins.
Røgen B, Ditlefsen C, Vangkilde-Pedersen T, Nielsen LH, Mahler A. Geothermal energy use, 2015 Country Update for Denmark. Proceedings World Geothermal Congress 2015, Melbourne; 2015.
Seibt P, Kellner T. Practical experience in the reinjection of cooled thermal waters back into sandstone reservoirs. Geothermics. 2003;32:733–41.
Stemmerik L, Frykman P, Christensen OW, Stentoft N. The Zechstein carbonates of southern Jylland. In: Brooks J, Glennie, KW, editors. Petroleum Geology of North West Europe; 1987. p. 365–74.
Texaco. Kegnæs-1 Completion Report Well 5410/5-1. Texaco; 1985.
Tiab D, Donaldson EC. Petrophysics. Theory and practice of measuring reservoir rock and fluid transport properties. Amsterdam: Elsevier; 2004.
Tanikawa W, Shimamoto T. Comparison of Klinkenberg-corrected gas permeability and water permeability in sedimentary rocks. Int J Rock Mech Min Sci. 2009;46(2):229–38.
Vadapalli U, Srivastava N, Vedanti N, Dimri VP. Estimation of permeability of a sandstone reservoir by a fractal and Monte Carlo simulation approach: a case study. Nonlin Process Geophys. 2014;21:9–18.
Vejbæk OV. Effects of asthenospheric heat flow in basin modellering exemplified with the Danish Basin. Earth Planet Sci Lett. 1989;95:97–114.
Vejbæk OV. Dybe strukturer i danske sedimentære bassiner. Geologisk Tidsskrift. 1997;4:1–31.
Vosgerau, H, Mathiesen, A, Andersen, MS, Boldreel, LO, Hjuler, ML, Kamla, E, Kristensen L, Laier, T, Pedersen, CB, Pjetursson, B, Nielsen, LH. A new WebGIS portal with geological and geophysical data for exploration of deep geothermal energy. Review of survey activities 2015. Geol Surv Denmark Greenl Bull; (in press).
Walderhaug O, Eliassen A, Aase NE. Prediction of permeability in quartz-rich sandstones Examples from the Norwegian shelf and the Fontainebleau sandstone. J Sediment Res. 2012;82:899–912.
Weibel R, Olivarius M, Kristensen L, Friis H, Hjuler ML, Kjøller C, Mathiesen A, Nielsen LH. Predicting permeability of low enthalpy geothermal reservoirs: a case study from the Upper Triassic–Lower Jurassic Gassum formation, Norwegian-Danish Basin; (submitted).
Wolfgramm M, Rauppach K, Seibt P. Reservoir-geological characterization of Mesozoic sandstones in the North German Basin by petrophysical and petrograpical data. Geol Wiss. 2008;36(4–5):249–65.